Circular RNAs correlate with DNA damage in ageing human placental tissue and in stillbirth

Keywords: stillbirth, placenta, pregnancy, ageing, DNA, circular RNA, double stranded breaks, senescence

Anya L. Arthurs[1,2*], Matilda R. Jackson[3,4,5], Dylan McCullough[1,2], Hamish S. Scott[3,4,6,7,8], Christopher P. Barnett[6,9], Stuart T. Webb[1,2,3], Melanie D. Smith[1,2], Tanja Jankovic-Karasoulos[1,2], Gustaaf A. Dekker[10], Claire T. Roberts[1,2].

[1] Flinders Health and Medical Research Institute, Flinders University, Adelaide, South Australia, Australia 5042

[2] College of Medicine and Public Health, Flinders University, Adelaide, South Australia, Australia 5042

[3] Department of Genetics and Molecular Pathology, SA Pathology, Adelaide, South Australia, Australia 5000

[4] Centre for Cancer Biology, an alliance between SA Pathology and University of South Australia, Adelaide, South Australia, Australia 5000

[5] Australian Genomics, Parkville, Victoria, Australia

[6] Adelaide Medical School, The University of Adelaide, Adelaide, South Australia, Australia

[7]ACRF Genomics Facility, Centre for Cancer Biology, an alliance between SA Pathology and University of South Australia, Adelaide, South Australia, Australia

[8] UniSA Clinical and Health Sciences, University of South Australia, Adelaide, South Australia, Australia

[9] Paediatric and Reproductive Genetics Unit, South Australian Clinical Genetics Service, Women's and Children's Hospital, North Adelaide, South Australia, Australia

[10] Department Obstetrics and Gynecology, Lyell McEwin Hospital, The University of Adelaide, Adelaide, South Australia.

* Corresponding author: anya.arthurs@flinders.edu.au

Graphical Abstract

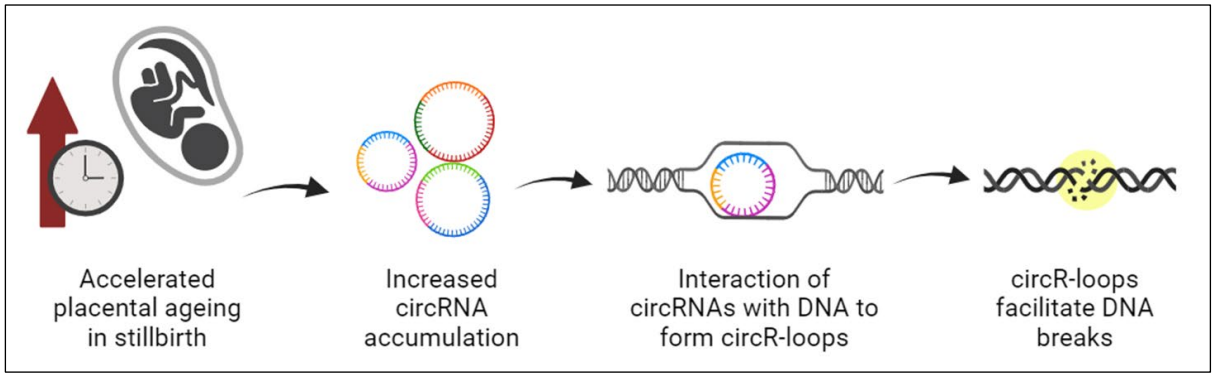

Abstract

Unexplained stillbirth may occur due to premature placental ageing, with unexpected deterioration of placental function for gestational age. Circular RNAs (circRNAs) are enzyme-resistant RNA molecules that accumulate in ageing tissues. Furthermore, circRNAs bind gDNA directly, forming circRNA:DNA complexes which can induce DNA breaks. This study investigated circRNA accumulation with gestational age in healthy and stillbirth placentae and determined whether circRNAs directly interact with placental DNA causing DNA damage.

Placenta samples (n=60 term uncomplicated; n=4 unexplained stillbirth) were assessed. Compared with earlier gestations (37, 38, 39, 40 weeks'), placental DNA damage and expression of 6 candidate circRNAs (circ_0009000, circ_0024157, circ_0061017, circ_0036877, circ_0054624 and circ_0111277), but not their linear transcripts, were increased in 40 and 41+ weeks' gestation samples, and in stillbirth. DRIP-qPCR signal size was significantly larger in term placentae than in enzyme-treated controls, confirming that all candidate circRNA loci bind to placental DNA. Depletion of circ_0009000 by specific siRNA in HEK293T cells, significantly reduced DNA damage compared to control, and increased expression of senescence-associated genes.

Stillbirth placentae show accelerated ageing with premature accumulation of candidate circRNAs at levels consistent with older gestation tissue. These circRNAs bind to DNA and circ_0009000 causes DNA breaks and senescence in placenta. Therefore, circRNAs play a role in placental ageing and associate with stillbirth, likely via DNA damage.

1. Introduction

Stillbirth is defined as a fetal death prior to birth of a baby of either (i) ≥20 completed weeks' of gestation or, (ii) ≥400g birthweight[1]. Annually there are 2 million stillbirths worldwide[2], with ~2300 occurring every year in Australia, at a rate unchanged for decades[1]. Whilst some cases of stillbirth can be attributed to fetal congenital abnormalities, many cases of stillbirth are "unexplained", where autopsy that includes fetal genetics does not establish cause. Although some risk factors have been identified[1,3], the aetiology of unexplained stillbirth is unknown, and is thus impossible to prevent. One theory for the mechanism underpinning unexplained stillbirth is premature placental ageing.

The placenta is a transient organ with a finite life in gestation. Placental ageing is a normal phenomenon resulting in physical changes in late gestation without fetal compromise. Accelerated placental ageing can occur in stillbirth, leading to reduced placental functional capacity for fetal support. Whilst markers of tissue ageing, including measures of DNA damage[3-5], are reportedly irregularly high in stillbirth placentae, a direct measure of DNA breaks has not previously been reported.

Tissue ageing has been associated with circular RNAs (circRNAs). circRNAs can be generated from most genes and encompass one or multiple exonic or intronic regions of RNA. Importantly, they display tissue-specific patterns of expression, making them unique to their tissue of origin as well as the genome of the individual. circRNAs are inherently stable, hence they can accumulate in tissues with age (previously shown in *Drosophila melanogaster, Caenorhabditis elegans* and murine models[6-8]).

Whilst circRNAs have many functions[9], of importance is their ability to directly bind to

genomic DNA, forming a circRNA:DNA complex (termed a 'circR-loop')[10]. Due to the steric hinderance, the presence of a circR-loop can cause RNA polymerase II to stall during transcription, subsequently leading to a DNA break. This often results in genomic instability[11], cellular senescence or apoptosis[12], and cell death[13].

Given that unexplained stillbirth may be due to premature placental ageing, and that circRNAs accumulate in ageing animal tissues, we sought to determine whether circRNAs accumulated with gestational age in healthy and stillbirth placentae. We accomplished this by quantifying RNA (both circRNA-enriched and total) to ensure no significant changes in transcript numbers with gestational age. We also quantified circRNA abundance along with all cognate linear transcripts for each circRNA, to ensure changes in circRNA abundances were due to accumulation, not simply products of alternative splicing. We further investigated whether select circRNAs bind to DNA to form circR-loops and induce DNA breaks. This study provides novel evidence of circRNA accumulation in ageing human tissue and proposes a potential mechanism for stillbirth pathogenesis.

2. Results

2.01 Cohort Characteristics

Placenta samples were available from n = 60 women who had healthy pregnancies (n = 12 per gestational group) and n = 4 women who experienced stillbirth. All stillbirths had been assessed by clinical pathologists as "unexplained fetal deaths", with no noted congenital anomalies. Maternal and birth characteristics are presented in **Table 1**.

2.02 DNA damage is increased in placentae from 40 and 41+ weeks' gestation, and in stillbirth

DNA damage was assessed using the Comet Assay that yields a Tail DNA% metric, an indication of the level of DNA damage in placental cells. Representative images of healthy cells (**Figure 1A**) and DNA damaged cells (**Figure 1B**) are included for reference. Tail DNA % was significantly higher in cells from placentae sampled at 40 weeks' gestation compared with 37 and 38 weeks' ($p_{37} = 0.0381$, $p_{38} = 0.0203$; **Figure 1C**). Tail DNA% was significantly higher in cells from placentae sampled at 41+ weeks' gestation compared with 37, 38, 39 and 40 weeks' (all $p < 0.0001$) as well as in placentae from stillbirths compared with 37, 38, 39 and 40 weeks' gestation ($p_{37} < 0.0001$, $p_{38} < 0.0001$, $p_{39} < 0.0001$, $p_{40} = 0.0001$).

2.03 Abundance of total RNA, and circRNA, is unchanged with gestation and in stillbirth

RNA concentration was measured in placenta samples from 37, 38, 39, 40 and 41+ weeks' gestation, and in placenta samples from stillbirths. RNA was extracted from each sample, then split into two aliquots; the first was untreated (total RNA) while the second was digested with RNase R (leaving only circRNAs). RNA concentration and abundance of total RNA and RNase R-digested RNA were assessed to determine whether these changed across gestation or in stillbirth.

Both RNA concentration (**Figure 2A-B**) and relative abundance level (**Figure 2C**) total RNA and RNase R-digested RNA was unchanged with gestation and in stillbirth.

2.04 Abundance of circ_0009000, but not linear *CRHR2* mRNA gene variants, is increased in placentae from 40 and 41+ weeks' gestation, and in stillbirth

Relative abundance of circ_0009000, expressed as fold change compared to abundance in placentae at 37 weeks' gestation, was significantly increased in cells from placentae sampled at 40 weeks' gestation compared with 37 and 38 weeks' ($p_{37} = 0.0005$, $p_{38} = 0.0079$; **Figure 3A**). circ_0009000 abundance was also significantly increased in cells from placentae taken at 41+ weeks' gestation compared with 37 and 38 weeks' (all $p < 0.0001$), as well as in placentae from stillbirths compared with 37 and 38 weeks' gestation ($p_{37} < 0.0001$, $p_{38} = 0.0006$).

Abundance of linear *CRHR2* mRNA (relative to *YWHAZ* and *ACTB*) was assessed for all gene variants (transcripts: XM_024446665.1 (**Figure 3B**), XM_017011752.2 (**Figure 3C**), NM_001202483.2 (**Figure 3D**), NM_001202482.2 (**Figure 3E**), NM_001202481.1 (**Figure**

3F) and NM_001202475 (**Figure 3G**)); for all transcripts, abundance was not significantly changed between groups.

2.05 Abundance of circ_0024157, but not linear *CWF19L2* mRNA gene variants, is increased in placentae from 40 and 41+ weeks' gestation, and in stillbirth

Relative abundance of circ_0024157, expressed as fold change on abundance levels in placentae at 37 weeks' gestation, was significantly increased in cells from placentae sampled at 40 weeks' gestation compared with 37 weeks' ($p = 0.0003$, **Figure 4A**). Relative abundance was also increased in cells from placentae sampled at 41+ weeks' gestation compared with 37, 38 and 39 weeks' ($p_{37} < 0.0001$, $p_{38} = 0.0002$, $p_{39} = 0.0124$), as well as in placentae from stillbirths compared with 37, 38 and 39 weeks' gestation ($p_{37} < 0.0001$, $p_{38} = 0.0027$, $p_{39} = 0.0336$).

Abundance of linear *CWF19L2* mRNA (relative to *YWHAZ* and *ACTB*) was assessed for all gene variants (transcripts: XM_017017239.2 (**Figure 4B**), XR_947795.2 (**Figure 4C**), NM_152434.3 (**Figure 4D**), and XM_011542620.3 (**Figure 4E**)); for all transcripts, abundance was not significantly changed between groups.

2.06 Abundance of circ_0061017, but not the linear *RAB22A* mRNA gene variants, is increased in placentae from 39, 40 and 41+ weeks' gestation, and in stillbirth

Relative abundance of circ_0061017, expressed as fold change on abundance levels in placentae at 37 weeks' gestation, was significantly increased in cells from placentae sampled

at 39 weeks' gestation compared with 37 weeks' (p = 0.0260; **Figure 4F**) and 40 weeks' gestation compared with 37 and 38 weeks' (p_{37} < 0.0001, p_{38} = 0.0053). Relative abundance was also increased in cells from placentae sampled at 41+ weeks' gestation compared with 37 and 38 weeks' (p_{37} < 0.0001, p_{38} = 0.0003), as well as in placentae from stillbirths compared with 37 and 38 weeks' gestation (p_{37} < 0.0001, p_{38} = 0.0034).

Abundance of linear *RAB22A* mRNA (relative to *YWHAZ* and *ACTB*) was assessed for the only gene variant (transcript: NM_020673.3 (**Figure 4G**); abundance was not significantly changed between groups.

2.07 Abundance of circ_0036877, but not linear *FURIN* mRNA gene variants, is increased in placentae from 39, 40 and 41+ weeks' gestation, and in stillbirth

Relative abundance of circ_0036877, expressed as fold change compared to abundance in placentae at 37 weeks' gestation, was significantly increased in cells from placentae sampled at 39 weeks' gestation compared with 37 weeks' (p = 0.0151; **Figure 5A**), and at 40 weeks' gestation compared with 37 weeks' (p = 0.0002). circ_0036877 abundance was significantly increased in cells from placentae taken at 41+ weeks' gestation compared with 37 and 38 weeks' (all p < 0.0001), as well as in placentae from stillbirths compared with 37 and 38 weeks' gestation (p_{37} < 0.0001, p_{38} = 0.0038).

Abundance of linear *FURIN* mRNA (relative to *YWHAZ* and *ACTB*) was assessed for all gene variants (transcripts: NM_001382622.1 (**Figure 5B**), NM_002569.4 (**Figure 5C**), NM_001382619.1 (**Figure 5D**), NM_001289823.2 (**Figure 5E**), NR_168464.1 (**Figure 5F**) NM_001382620.1 (**Figure 5G**), NM_001382621.1 (**Figure 5H**) and NM_001289824.2 (**Figure 5I**)); for all transcripts, abundance was not significantly changed between groups.

2.08 Abundance of circ_0054624, but not the linear *PNPT1* mRNA gene, is increased in placentae from 40 and 41+ weeks' gestation, and in stillbirth

Relative abundance of circ_0054624, expressed as fold change compared to abundance in placentae at 37 weeks' gestation, was significantly increased in cells from placentae sampled at 40 weeks' gestation compared with 37 and 38 weeks' ($p_{37} < 0.0001$, $p_{38} = 0.0232$; **Figure 6A**). circ_0054624 abundance was significantly increased in cells from placentae taken at 41+ weeks' gestation compared with 37, 38 and 39 weeks' ($p_{37} < 0.0001$, $p_{38} < 0.0001$, $p_{39} = 0.0138$), as well as in placentae from stillbirths compared with 37 and 38 weeks' gestation ($p_{37} < 0.0001$, $p_{38} = 0.0012$).

Abundance of linear *PNPT1* mRNA (relative to *YWHAZ* and *ACTB*) was assessed for the only gene variant (transcript: NM_033109.5 (**Figure 6B**)); abundance was not significantly changed between groups.

2.09 Abundance of circ_0111277, but not the linear *PAPPA2* mRNA gene, is increased in placentae from 39, 40 and 41+ weeks' gestation, and in stillbirth

Relative abundance of circ_0111277, expressed as fold change compared to abundance in placentae at 37 weeks' gestation, was significantly increased in cells from placentae sampled at 39 weeks' gestation compared with 37 weeks' ($p = 0.0443$; **Figure 6C**) and in cells from placentae sampled at 40 weeks' gestation compared with 37 weeks' ($p = 0.0002$. circ_0111277 abundance was significantly increased in cells from placentae taken at 41+ weeks' gestation compared with 37, 38 and 39 weeks' ($p_{37} < 0.0001$, $p_{38} < 0.0001$, $p_{39} = 0.0158$), as well as in

placentae from stillbirths compared with 37 and 38 weeks' gestation ($p_{37} < 0.0001$, $p_{38} = 0.0042$).

Abundance of linear *PAPPA2* mRNA (relative to *YWHAZ* and *ACTB*) was assessed for the only gene variant (transcript: XM_005245422.3 (**Figure 6D**)); abundance was not significantly changed between groups.

2.10 circRNAs circ_0009000, circ_0024157, circ_0061017, circ_0036877, circ_0054624 and circ_0111277 bind to DNA to create circR-loops in term placentae

DRIP-qPCR was used to detect circR-loops (DNA:RNA complexes) in pooled samples of gestations 37-41+ weeks', to determine whether circRNAs which accumulate in the ageing placenta interact directly with DNA.

After completing DRIP (see Methods) DRIP-qPCR analysis was undertaken using either predesigned primers[14] for known R-loop-positive loci *TFPT* and *CALM3*, and known R-loop-negative locus *EGFR1neg*, or using custom-designed primers (sequences listed in Methods) to target the backsplice junctions of circ_0009000, circ_0024157, circ_0061017, circ_0036877, circ_0054624 and circ_0111277. All DRIP-qPCR analyses were completed both in samples treated with and without RNase H treatment prior to DRIP. As RNase H cleaves the RNA of RNA:DNA hybrids, it is expected that addition of RNase H to the sample will result in a significantly suppressed R-loop signal and hence, a reduced DRIP-qPCR signal (functioning as a negative control). This was confirmed in our results.

According to Sanz, *et al.*[14], R-loop positive loci are typically recovered with an efficiency ranging from 1-15% of total input, whereas negative loci are typically recovered with values of <0.1%. This was replicated in our results for placenta tissue **(Figure 7A)**, where *TFPT* (mean 11.499%, $p = 0.0008$) and *CALM3* (mean 8.644%, $p = 0.0009$) produced DRIP-qPCR signals, shown as a % of total DRIP input, significantly larger than their RNase H-treated controls. There was no significant difference between the DRIP-qPCR signals of *EGFR1neg* (mean 0.389%) with and without RNase H treatment.

DRIP-qPCR signal for circ_0009000 (mean 0.173%, $p < 0.0001$; **Figure 7B**), circ_0024157 (mean 0.166%, $p < 0.0001$), circ_0061017 (mean 0.172%, $p < 0.0001$), circ_0036877 (mean 0.169%, $p < 0.0001$), circ_0054624 (mean 0.173%, $p < 0.0001$) and circ_0024157 (mean 0.177%, $p < 0.0001$) was significantly larger than their RNase H-treated controls.

2.11 DNA damage is mitigated with depletion of circ_0009000

circR-loops introduce steric hinderance with the formation of the circRNA:DNA hybrid, which can promote transcriptional pausing and subsequent DNA breaks[15-17], resulting in genomic instability[18]. As such, we investigated whether circ_0009000, in forming a circR-loop, induces DNA damage. This was confirmed using a custom-designed circ_0009000-specific siRNA in HEK293T cells.

Validation of the siRNA knockdown

Cultured HEK293T cells were either untreated (control), treated with a scrambled siRNA or with a custom-designed siRNA specific to circ_0009000. Cells were then cultured for 72 hours prior to harvesting for qPCR analysis (**Figure 8A**) as well as Comet Assay analysis (**Figure 8B**).

As shown in **Figure 8A**, transfection with the scrambled siRNA did not alter the expression of the linear *CRHR2* mRNA (shown as abundance relative to *YWHAZ* and *ACTB*) compared to control. Importantly, administration of the siRNA specific to circ_0009000 did not alter the expression of linear *CRHR2* mRNA. However, administration of the siRNA successfully reduced the relative abundance of circ_0009000 compared with both the untreated cells (control) and cells treated with the scrambled siRNA (all $p < 0.0001$).

Quantification of DNA damage in circ_0009000-depleted HEK293T cells

Transfection with the siRNA specific to circ_0009000 in HEK293T cells significantly reduced the level of DNA damage (tail DNA%) compared with both the control (reduced by 41.3%) and scrambled (reduced by 39.5%) groups (all $p < 0.0001$). Transfection with the scrambled siRNA in HEK293T cells did not alter the level of DNA damage (tail DNA%) compared with the control, indicating that depletion of circ_0009000 results in reduced DNA damage.

2.12 Expression of senescence-associated genes is attenuated with depletion of circ_0009000

Saul *et al.*[19] validated a gene set which identifies senescent cells and predicts senescence-associated pathways in tissue. mRNA expression of these senescence-associated genes (**Figure 9A**) was significantly decreased in cells transfected with the siRNA specific to circ_0009000 compared to control; *CXCL8* ($p = 0.0053$), *CCL3* ($p = 0.0291$), *CTSS* ($p < 0.0001$), *AIF1* ($p < 0.0001$), *HMGA1* ($p < 0.0001$) and *HIRA* ($p = 0.0005$). mRNA expression of *CST3*, *TYROBP*, *FCER1G* and *LYZ* was not significantly changed.

2.13 Expression of senescence-associated genes is increased in 41+ weeks' gestation healthy and stillbirth tissue compared with 37 weeks' gestation healthy placenta tissue

mRNA expression of senescence-associated genes (**Figure 9B**) as described by Saul *et al.*[19] was significantly increased in 41+ weeks' gestation healthy placentae ($p_{CXCL8} < 0.0001$; $p_{CST3} < 0.0001$; $p_{TYROBP} < 0.0001$; $p_{FCER1G} < 0.0001$; $p_{LYZ} < 0.0001$; $p_{CCL3} < 0.0001$; $p_{CTSS} < 0.0001$; $p_{AIF1} < 0.0001$; $p_{HMGA1} < 0.0001$; $p_{HIRA} < 0.0001$) and stillbirth placentae ($p_{CXCL8} < 0.0001$; $p_{CST3} < 0.0001$; $p_{TYROBP} = 0.0003$; $p_{FCER1G} < 0.0001$; $p_{LYZ} < 0.0001$; $p_{CCL3} < 0.0001$; $p_{CTSS} < 0.0001$; $p_{AIF1} < 0.0001$; $p_{HMGA1} < 0.0001$; $p_{HIRA} < 0.0001$) compared with 37 weeks' gestation healthy placentae.

mRNA expression of *TYROBP* was significantly increased in 41+ weeks' gestation healthy placentae compared with stillbirth placentae ($p = 0.0038$). mRNA expression of *CXCL8, CST3, FCER1G, LYZ, CCL3, CTSS, AIF1, HMGA1* and *HIRA* was not significantly changes between groups.

3. Discussion

Like other tissues in the body, the placenta undergoes the normal phenomenon of ageing. Tissue ageing includes progressive increases in cellular senescence[20]. For the placenta, this implies a decline in functionality as gestational age increases, resulting in a reduced capacity of the placenta to support the fetus[3]. Placentae from stillbirths undergo an accelerated ageing process[3], exhibiting similar pathological features regardless of their earlier gestational ages. Markers of ageing such as increased DNA and RNA oxidation, lipid peroxidation, altered perinuclear location of lysosomes and larger autophagosomes are found in placentae from stillbirths as well as those from healthy late term compared with placentae from healthy early term[3]. In this study we provide new and compelling evidence to support the notion of premature placental ageing in stillbirth, as we found increased DNA breaks in placentae from stillbirths and those from healthy late term (40, 41+ weeks' gestation) compared with those from early term (37-39 weeks').

Our group 41+ weeks' gestation encompassed women who birthed between 41+1 and 41+6 weeks'. Given that gestation of >40 weeks, in addition to maternal age ≥35 years[3] and male fetal sex[1], are risk factors for stillbirth, the Australian Pregnancy Care Guidelines consider 42 weeks' and beyond as post-term and recommend fetal monitoring and induction of labour from 41 weeks', even in uncomplicated, low risk patients[21]. Indeed, evidence shows that stillbirth and neonatal death can be reduced with fetal surveillance twice weekly from 39 weeks'[22]. This study confirmed that rates of DNA damage in placentae from 41+ weeks' gestation were significantly increased compared to earlier term gestations. Placentae from stillbirths had further elevated DNA damage, although this was not statistically significant from those at 41+ weeks' potentially due to the small sample size. As our stillbirth placentae were collected at gestational weeks 23, 26, 31 and 34, and DNA damage is a recognised marker of tissue

ageing[23], this clearly indicates that in stillbirth the placenta experiences accelerated tissue ageing, resulting in a post-term phenotype much earlier than would be appropriate for their gestational age.

The accumulation of circRNAs in aged tissue is a relatively recent discovery. Preliminary evidence for this was uncovered from RNA-seq libraries from *Drosophila melanogaster*, where expression of >200 circRNAs were significantly increased in the heads of 20-day old flies, compared with 1-day old flies[6]. Accumulation of circRNAs with ageing has also been evident in studies[24] using *Drosophila melanogaster* photoreceptor neurons[25], mouse brain and heart[8] and *Caenorhabditis elegans*[7]. It is most likely that circRNAs accumulate in tissues as their lack of a 5' cap and polyadenylated tail renders them resistant to exoribonuclease degradation[26]. Another explanation for circRNA accumulation in some tissues is that in cell types such as neurons, rates of mitosis and proliferation are lower than other cell types, allowing reduced turnover of circRNAs[24,27-29]. Given that the nuclei of the syncytiotrophoblast are non-mitotic[30], transcription is significantly reduced[31] and the syncytiotrophoblast displays markers of senescence[32,33], this could be a primary area of circRNA accumulation.

Recently, circRNAs were identified as a potential forensic tool for estimating biological age using a panel of 5 circRNAs which accumulate in human blood[34], which is an exciting leap from circRNA accumulation in animals to differential circRNA expression with age in humans. Other studies have shown differentially expressed circRNAs in human granulosa cells from women who were young versus those of advanced reproductive age[35], and that specific circRNAs in human peripheral blood were associated with parental longevity and cellular senescence[36]. The link between circRNA differential expression and Alzheimer's disease is becoming more widely investigated[37], which is of particular interest to this study given that

Alzheimer's disease is, at its core, an ageing disorder[38]. Whilst these studies demonstrate that expression of circRNAs is *changed* between differently aged groups, none of these studies investigated circRNAs *accumulation* in ageing tissue.

The abundance of a circRNA is a combination of expression level as well as accumulation. circRNA expression level can be increased by overexpressing the linear gene, or by alternative splicing that promotes the circular over the linear transcript(s). circRNA accumulation indicates that the circRNA remains in the tissue[24], unaffected by exoribonucleases[26]. Over time, the abundance of the circRNA in the tissue increases as the accumulated transcripts escape degradation. This occurs without change in the linear gene expression nor alternative splicing. The result is that these circRNAs can continually exert their function in the tissue well after their linear gene's expression and at higher-than-expected abundance.

As an organ that undergoes a well-characterised ageing process during gestation, we hypothesised that the placenta may also experience circRNA accumulation with tissue ageing. In this study, we report the first evidence of circRNA accumulation in human tissue. circRNAs circ_0009000, circ_0024157, circ_0061017, circ_0036877, circ_0054624 and circ_0111277 were all increased in abundance in human placentae from late term (40, 41+ weeks') compared with early term (37, 38, 39 weeks'), while abundance of their cognate linear mRNAs were unchanged. Furthermore, we found no evidence of changed alternative splicing patterns, as indicated by absence of differential expression of gene variants between gestational weeks. This indicates that the excess levels of these candidate circRNAs found in late term compared with early term placentae were not the product of increased gene expression, nor the product of a switch to a different dominant isoform of the gene which may result in production of a circular transcript. Hence, we can conclude that these candidate circRNAs accumulate in the tissue as gestation continues and the organ ages.

To our knowledge, ours is the first study to confirm that circRNAs accumulate in human aged tissue. Importantly, we established that there is no global increase in total RNA, nor circular RNA, abundance with placental gestational age. This confirms that our candidate circRNAs are unique in their ability to accumulate with age. It should be noted that accumulation of these specific circRNAs with age may be placenta-specific, as this study only examined placental tissue, and this candidate list may not be exhaustive. Further studies will profile all accumulating circRNAs in the placenta as it ages.

Due to the low abundance of the candidate circRNAs, we investigated their interaction with DNA as a stoichiometrically favourable potential function (given that there are only 2 copies of DNA per cell, compared with thousands of copies of microRNAs and proteins). By performing DRIP on RNA which was later treated with RNase R to degrade linear transcripts, this allowed isolation of circRNA moieties that bind placental DNA. DRIP-qPCR analysis showed that circRNAs circ_0009000, circ_0024157, circ_0061017, circ_0036877, circ_0054624 and circ_0111277, which accumulate with gestational age and in stillbirth, also form circR-loops in term placentae.

A circR-loop is formed when a circRNA molecule binds one strand of helicase-unwound genomic DNA[10]. The steric hindrance of this bulky structure causes RNA polymerase II to stall during transcription, resulting in a DNA break, and often a subsequent fusion at another locus[39], promoting genomic instability[11]. Double-stranded DNA breaks are lethal to cells, as they affect both strands of DNA and promote the loss of genetic information[13]. Any type of DNA damage can trigger cellular apoptosis or senescence[12]. Given that we observed increased DNA breaks in stillbirth placentae, which also had elevated abundance of circ_0009000, we utilised a

circ_0009000 knockdown model in HEK293T cells to determine whether presence of this circRNA was associated with induction of DNA damage.

Results from this study indicate that targeted knockdown of circ_0009000 with an siRNA reduces double-stranded DNA damage in HEK293T cells. Importantly, this occurred in the absence of any change in the linear mRNA expression, indicating that this is a circRNA-specific result. While this finding does not elucidate a molecular mechanism for circ_0009000 induction of DNA damage, nor does it indicate that this occurs in the human placenta *in vivo*, it provides compelling evidence to further support the hypothesis that circ_0009000 causes DNA breaks by forming circR-loops with placental DNA. This represents an important avenue for further investigation, with therapeutic potential in reducing circRNAs accelerating placental ageing. Indeed, the use of, and targeted inhibition of, circRNAs as a therapeutic option is growing[40-43].

circ_0009000 is formed by non-canonical splicing of *CRHR2*, the gene for corticotrophin releasing hormone receptor 2 (CRHR2). Corticotrophin releasing hormone (CRH) production in the placenta is largely in the second and third trimesters of pregnancy[44], with CRH playing a critical role in parturition. Most CRH is secreted into the maternal bloodstream[45], however CRH receptors 1 (CRHR1) and 2 (CRHR2) (and their various isoforms) can be found in the placenta, with immunohistochemical staining localising CRHR2 mainly to the syncytiotrophoblast[46]. As circ_0009000 forms a circR-loop in placenta, binding its cognate locus, it is possible that this inhibits the translation of *CRHR2*, reducing availability of CRHR2 for CRH binding. Indeed, one study noted a significant downregulation in *CRH* mRNA expression in placentae from idiopathic stillbirths compared with live births[47], implying that

CRH mRNA may be downregulated to produce less CRH protein, which coheres with reduced availability of CRHR2 for binding.

Many other circRNAs this study confirmed to form circR-loops in placenta were also from genes that encode important proteins in placental function and pregnancy. *FURIN* encodes a pro-protein convertase that facilitates placental syncytialisation in first trimester trophoblasts[48], and *PAPPA2* encodes a metalloproteinase which cleaves Insulin Growth Factor (IGF) Binding Protein-3 and -5 (IGFBR3, IGFBP5), liberating IGF-1 for binding to membrane receptors[49]. Further investigations should assess whether circ_0036877 and circ_0111277 (from *FURIN* and *PAPPA2*, respectively) binding at their cognate loci reduce production of their respective encoded proteins. Indeed, there is evidence to suggest that FURIN is mainly associated with functions in early gestation[50]. Conversely, abnormally low PAPPA2 expression at term is associated with fetal growth restriction in humans[51], and *PAPPA2* knockout mice experience postnatal growth retardation and elevated total IGF-1[52].

Importantly, this study confirms that targeted circ_0009000 knockdown results in reduced expression of senescence-associated genes, thereby establishing a link between circ_0009000 and cellular senescence. This finding was recapitulated in primary tissue samples, with healthy late term placenta tissue and stillbirth placenta tissue expressing increased mRNA of senescence-associated genes compared with healthy early term placenta tissue. This confirms reports that the placenta has increased rates of cellular senescence with advancing gestation[53] and that unexplained stillbirth placentae experience premature ageing, thus leading to higher rates of cellular senescence[54]. Taken together, our experimental findings suggest that circ_0009000, which we have confirmed to physically bind to placental DNA, causes DNA

breaks contributing to cellular senescence. This presents a promising avenue for investigation as a mechanism for stillbirth via premature placental ageing.

To summarise, this study provides evidence that (a) multiple circRNAs accumulate in human aged placental tissue and stillbirth placentae, (b) these circRNAs bind to DNA in the human term placenta to form circR-loops and (c) circ_0009000 has the capacity to facilitate DNA damage and increase senescence in human cells. We propose the following mechanism as a potential contributor to stillbirth pathology (**Figure 10**): In uncomplicated pregnancy, circRNAs naturally accumulate in placental cells as the tissue ages with gestation. However, in pregnancies resulting in unexplained stillbirth, premature placental ageing results in accelerated accumulation of circRNAs. These circRNAs form circRNA:DNA complexes in the placenta, with at least one circRNA (circ_0009000) known to facilitate DNA damage and induce senescence. As DNA breaks facilitate genomic instability[11] and cellular senescence[55] and apoptosis[56], this may result in reducing placental function to the detriment of the fetus.

A limitation of this study is the small sample size of stillbirth placentae; however, this is a common issue in stillbirth research[3,57] given the difficulty in obtaining tissue within an appropriate timeframe. As stillbirths that could be explained by fetal congenital abnormality were excluded, resulting in a pure “unexplained stillbirth” sample pool, this further reduced available tissue samples. Moreover, sample size limited our ability to perform fetal sex-specific statistical tests. Further studies will be conducted with larger sample sizes to allow for increased comparisons. Future studies will also include participants of different ethnicities, accounting for ethnicities which are more prone to stillbirths (such as South Asian women[22]).

Here, we present the first report of circRNA accumulation in ageing human placental tissue, in the absence of any change in total linear or circular RNA expression nor alternative splicing variants. Importantly, circRNAs circ_0009000, circ_0024157, circ_0061017, circ_0036877, circ_0054624 and circ_0111277 are present at exceptionally high levels in placenta from stillbirths, similar to or surpassing the circRNA levels found in post-term placentae. Furthermore, our study provides evidence that these circRNAs bind to DNA to form circR-loops in placental tissue. Finally, our *in vitro* experiments show that knockdown of circ_0009000 results in decreased DNA breaks in cells, indicating that this circRNA facilitates DNA damage, and decreased expression of senescence-associated genes, implying that this circRNA induces cellular senescence.

4. Methods

4.01 Tissue Samples

Healthy placentae from 37-41+ weeks' gestation: Term placentae were obtained at the Lyell McEwin Hospital in Elizabeth, South Australia, from women recruited as part of the Screening Tests to predict poor Outcomes of Pregnancy (STOP) (2015–2018) cohort study[58]. The study was registered with the Australian and New Zealand Clinical Trials Registry (ACTRN 12614000985684). All placentae were associated with uncomplicated pregnancies and were collected from white women. Tissue biopsies from placentae were washed in phosphate-buffered saline (PBS) before being snap frozen and held in liquid nitrogen for 15 min, then stored at -80°C. Ethics approval was obtained from the Women's and Children's Health Network Human Research Ethics Committee (HREC/14/WCHN/90; STOP). All women provided written informed consent.

Placentae collected from unexplained stillbirths: Small placental biopsies from unexplained stillbirth cases were obtained from women who had been recruited in to the NHMRC- and GHFM-MRFF-funded Genomic Autopsy Study[59]. Placental biopsies were obtained as part of the standard autopsy procedure and were stored at -80°C as approved by the Human Ethics Committee of the Women's and Children's Health Network, South Australia, Australia (HREC/15/WCHN/35) and Melbourne Health as part of the Australian Genomics Health Alliance protocol (HREC/16/MH/251). Informed consent was obtained to allow access to relevant medical information and subsequent storage of anonymized samples, genomic data and/or medical information in relevant databases and publications.

4.02 RNA Extraction

Healthy term and stillbirth placental tissues (25mg) were weighed and washed with phosphate-buffered saline (PBS). Tissue was disrupted by homogenizing for 3.5 min at 30 Hz (TissueLyser, QIAGEN) in 1mL *TRIzol Reagent* (Sigma-Aldrich). The manufacturer's protocol was then followed to isolate total RNA. The purity and integrity of extracted RNA samples were determined using the Experion™ (BioRad) and samples used had an RNA Quality Index ≥ 8. Samples were split into two aliquots, with one aliquot to be assessed for circRNA expression levels and the other to be assessed for linear transcript expression levels. Samples to be assessed for circRNA expression levels were heated to 70°C for 5 mins, then immediately cooled below 40°C before incubation with RNase R (10U / reaction; Astral Scientific) for 1 h at 40°C. This step was essential to digest all linear RNAs, leaving only lariat or circular RNA structures.

4.03 RNA Quantification

Total RNA for each sample, after incubation of 1 µg of RNA either with RNase R or untreated, was quantified using the Qubit 2.0 fluorimeter (Thermo Fisher Scientific). As per Drula, *et al.*[60], Qubit measurement was accomplished with the Qubit™ RNA High Sensitivity (HS) assay kit using 1 µL of the RNA sample, 198 µL of the kit Qubit working solution and 1 µL of the provided fluorophore, as per manufacturer's instructions. RNA amount was normalised based on the standard curve and input and compared between RNase R treated and untreated groups per sample to quantify bulk circRNA abundance.

4.04 cDNA Synthesis and Quantitative Polymerase Chain Reaction (qPCR)

Synthesis of complementary DNA (cDNA) was conducted beginning with 1µg of total RNA using the QuantiNova Reverse Transcription Kit (QIAGEN) according to the manufacturer's protocol. qPCR was performed in triplicate and conducted with SYBR Green (QIAGEN) according to manufacturer's instructions, with *YWHAZ, GAPDH* and *ACTB* as housekeeping genes (all primer sequences in **Table 2**). Custom divergent primers were designed for each circRNA, flanking the backsplice junction, with an amplicon size <300 base pairs. As an additional confirmation of amplification specificity, all primers were assessed using the Primer design BLAST tool[60]. Furthermore, primer specificity was confirmed via melt curve analysis from qRT-PCR. The qPCR conditions were PCR initial activation at 95°C for 5 min followed by 50 cycles of 95°C for 15s, T_m (detailed in **Table 2**) for 40s and 72°C for 20s. qPCR results were analysed using the 2-ΔΔCT method[61]. Samples were sorted into groups depending on gestational age of tissue (see **Table 1** for numbers and characteristics of women's samples used).

4.05 Cell culture and siRNA transfection

HEK293T cells (CRL-3216; ATCC) were cultured (n = 3, in triplicate; final n = 9) at 37°C in 5% CO_2 using Dulbecco's Modified Eagle Medium with GlutaMAX supplement (Gibco) and 10% v/v fetal bovine serum (Sigma-Aldrich). siRNA was produced by Thermo Fisher Scientific (Silencer Select siRNA). siRNA sequence was designed to be complementary to the backsplice junction of circ_0009000 (sequence: CTGCTCCACGGCTTGGCCACCTGTTCCCA; scrambled siRNA sequence: GACCTCGTGCTCGTCACCTCCGACTCGTC). Cells were transfected (24-well plates) with the siRNA and scrambled siRNA at 5, 10 and 20 nM final concentrations using Lipofectamine RNAiMAX (Life Technologies) following the manufacturer's instructions. After optimisation,

experiments proceeded with 10 nM final concentration (as the lowest siRNA concentration producing the desired level of knockdown). At 96 hours post-siRNA transfection cells were collected and either (i) immediately used for Comet assay or (ii) snap frozen in liquid nitrogen prior to storage at −80°C for subsequent RNA analysis.

4.06 Comet Assay

The Abcam Comet Assay Kit (ab238544; Abcam) was used to assess DNA damage in isolated trophoblasts. Approximately 25mg tissue (stored at -80°C) in 1.5mL ice-cold PBS containing 20 mM EDTA (without Mg^{2+} and Ca^{2+}) was minced using dissection scissors. The tissue suspension settled for 5 min (4°C) prior to removal of the supernatant for centrifugation (700xg, 2 min). The supernatant was then discarded, and the cell pellet was resuspended at $1x10^5$ cells/mL in ice-cold PBS (without Mg^{2+} and Ca^{2+}). Cell samples were combined with Comet Agarose at a 1/10 (v/v) ratio, mixed by pipetting and transferred onto pre-prepared Comet Agarose glass slides. Slides were incubated (in the dark, 15 min, 4°C) prior to immersion in Lysis Buffer (14.6g NaCl, 20 mL EDTA [provided], 10 mL 10X Lysis Solution [provided], 10 mL DMSO, volume adjusted to 90 mL with deionised H_2O, pH = 10.0) for 45 min (in the dark, 4°C). Slides were then transferred and immersed in Alkaline Solution (1.2g NaOH, 0.2 mL EDTA [provided], volume adjusted to 100 mL with deionised H_2O) for 30 min (in the dark, 4°C).

Alkaline electrophoresis was then performed as follows: slides were carefully transferred from the Alkaline Solution into the electrophoresis chamber containing Alkaline Electrophoresis Solution (1L of 300 mM NaOH, 1 mM EDTA; pH > 13, 4°C) and electrophoresis conditions applied (30V, 300mA, 30 min). Following electrophoresis, slides were carefully washed by

immersion in deionised H_2O (3 washes at 2 min each; 4°C) prior to submersion in 70% EtOH (5 min, 4°C), then dried at room temperature. Slides were visualised by staining with the supplied Vista Green DNA Dye and imaged by epifluorescence microscopy using a FITC filter.

The DNA integrity of 100 cells per placenta was analysed using CometScore 2.0 software (RexHoover.com). The fluorescence intensity of the comet 'tail' was used as a measure of DNA damage (indicated as tail DNA%). Tail DNA was shown as a percentage increase in damage relative to averaged control samples.

4.07 DNA:RNA ImmunoPrecipitation (DRIP)

DRIP was performed according to steps 3-25 in the protocol published by Sanz, *et al.* 2019[14], with some notable exceptions. As tissue was used as a starting material instead of cultured cells, tissue was first prepared as follows before progressing to step 3 of the protocol.

About 50mg frozen placental villous tissue was submerged in 1mL RLT+ buffer (QIAGEN) with added 0.01% (v/v) β-mercaptoethanol and 0.5% (v/v) Reagent DX (QIAGEN) with 1g beads. Tissue was disrupted by homogenizing for 3.5 min at 30 Hz (TissueLyser, QIAGEN). Cell suspensions were centrifuged (3 min, max speed, 4°C) prior to removal of the supernatant. The cell pellet was washed (sterile DPBS, 5mL) before centrifugation (3 min, 1000 RPM, 4°C) and removal of the supernatant. Steps 3-25 of the protocol[14] were then followed.

4.08 Statistical Analysis

Statistical analysis for differences between groups for qPCR and Comet Assay data was undertaken using SPSS Statistics Software. Outliers were removed from the data using a Grubbs' test. Data were assessed for normality distribution and either a Kruskal-Wallis test or two-way ANOVA tests conducted. Adjustments were made for multiple comparisons (Tukey's). Differences between groups were considered significant at $p < 0.05$.

Competing Interest Statement

Provisional patent # 2024902762, filed 2nd September 2024.

Acknowledgments

We thank the women who consented to their placental tissue being used for this research. Thank you to the clinical and anatomical staff from the Women's and Children's Hospital and Lyell McEwin Hospital who were involved in the women's care, and who collected and biopsied the placental samples. Figures were created using Biorender.com

Author Contributions

A.L.A. conceptualised this work, performed experimental work and formal analysis of data, original draft preparation, and review and editing. M.R.J., H.S.S. and C.P.B. provided stillbirth placenta samples and reviewed and edited the manuscript. D.M. contributed to experimental work and data analysis. S.W. provided molecular expertise and reviewed and edited the manuscript. M.D.S. and T.J-K. reviewed and edited the manuscript. G.A.D. provided clinical expertise and reviewed and edited the manuscript. C.T.R. provided supervision, funding acquisition, interpretation of data, review and editing of the manuscript. All authors contributed to the article and approved the final version.

Funding

A.L.A. is supported by funding from the Flinders Foundation, Flinders University and the Channel 7 Children's Research Foundation.

C.T.R. is supported by an NHMRC Investigator Grant (GNT1174971) and a Matthew Flinders Fellowship from Flinders University.

The Genomic Autopsy Study was supported by NHMRC (#APP1123341), Genomics Health Futures Mission – Medical Research Futures Fund (#GHFM76777) and the Australian Genomic Health Alliance NHMRC Targeted Call for Research into Preparing Australia for the Genomics Revolution in Healthcare (#GNT1113531) to H.S.S. and C.P.B.

References

1 (ed Australian Institute of Health and Welfare) (Australian Institute of Health and Welfare, 2018).

2 Hug, L., You, D., Blencowe, H., Mishra, A., Wang, Z. *et al.* Global, regional, and national estimates and trends in stillbirths from 2000 to 2019: a systematic assessment. *The Lancet* **398**, 772-785 (2021).

3 Maiti, K., Sultana, Z., Aitken, R. J., Morris, J., Park, F. *et al.* Evidence that fetal death is associated with placental aging. *Am J Obstet Gynecol* **217**, 441 (2017).

4 Amir, H., Weintraub, A., Aricha-Tamir, B., Apel-Sarid, L., Holcberg, G. *et al.* A piece in the puzzle of intrauterine fetal death: pathological findings in placentas from term and preterm intrauterine fetal death pregnancies. *The journal of maternal-fetal & neonatal medicine* **22**, 759-764 (2009).

5 Ferrari F, F. F., Saade G, Menon R. Placental telomere shortening in stillbirth: a sign of premature senescence? *Journal of Maternal-Fetal and Neonatal Medicine* **29**, 1283-1288 (2016). https://doi.org/DOI: 10.3109/14767058.2015.1046045

6 Westholm, J. O., Miura, P., Olson, S., Shenker, S., Joseph, B. *et al.* Genome-wide analysis of drosophila circular RNAs reveals their structural and sequence properties and age-dependent neural accumulation. *Cell reports* **9**, 1966-1980 (2014).

7 Cortes-Lopez M, G. M., Cooper DA, Gruner HN, Voda AI, van der Linden AM, Miura P. Global accumulation of circRNAs during aging in Caenorhabditis elegans. *BMC Genomics* **19** (2018).

8 Gruner H, C.-L. M., Cooper DA, Bauer M, Miura P. . CircRNA accumulation in the aging mouse brain. *Sci Rep* **6**, 38907 (2016).

9 Arthurs, A. L., Jankovic-Karasoulos, T., Smith, M. D. & Roberts, C. T. Circular RNAs in Pregnancy and the Placenta. *International Journal of Molecular Sciences* **23**, 4551 (2022).

10 Conn, S. J., Pillman, K. A., Toubia, J., Conn, V. M., Salmanidis, M. *et al.* The RNA binding protein quaking regulates formation of circRNAs. *Cell* **160**, 1125-1134 (2015).

11 Lord, C. J. & Ashworth, A. The DNA damage response and cancer therapy. *Nature* **481**, 287-294 (2012).

12 Parrinello, S., Coppe, J.-P., Krtolica, A. & Campisi, J. Stromal-epithelial interactions in aging and cancer: senescent fibroblasts alter epithelial cell differentiation. *Journal of cell science* **118**, 485-496 (2005).

13 Altaf, M., Saksouk, N. & Côté, J. Histone modifications in response to DNA damage. *Mutation Research/Fundamental and Molecular Mechanisms of Mutagenesis* **618**, 81-90 (2007).

14 Sanz, L. A. & Chédin, F. High-resolution, strand-specific R-loop mapping via S9. 6-based DNA–RNA immunoprecipitation and high-throughput sequencing. *Nature protocols* **14**, 1734-1755 (2019).

15 El Hage, A., Webb, S., Kerr, A. & Tollervey, D. Genome-wide distribution of RNA-DNA hybrids identifies RNase H targets in tRNA genes, retrotransposons and mitochondria. *PLoS genetics* **10**, e1004716 (2014).

16 Alexander, R. D., Innocente, S. A., Barrass, J. D. & Beggs, J. D. Splicing-dependent RNA polymerase pausing in yeast. *Molecular cell* **40**, 582-593 (2010).

17 Wongsurawat, T., Jenjaroenpun, P., Kwoh, C. K. & Kuznetsov, V. Quantitative model of R-loop forming structures reveals a novel level of RNA–DNA interactome complexity. *Nucleic acids research* **40**, e16-e16 (2012).

18 Conn, V. M., Gabryelska, M., Toubia, J., Kirk, K., Gantley, L. *et al.* Circular RNAs drive oncogenic chromosomal translocations within the MLL recombinome in leukemia. *Cancer cell* **41**, 1309-1326. e1310 (2023).
19 Saul, D., Kosinsky, R. L., Atkinson, E. J., Doolittle, M. L., Zhang, X. *et al.* A new gene set identifies senescent cells and predicts senescence-associated pathways across tissues. *Nature communications* **13**, 4827 (2022).
20 Holt, D., Grainger, DW. Senescence and quiescence induced compromised function in cultured macrophages. *Biomaterials* **33**, 7497-7507 (2012).
21 Australian_Government_Department_of_Health. (ed Department of Health) (Canberra, 2020).
22 Davies-Tuck, M. L., Davey, M.-A., Hodges, R. L. & Wallace, E. M. Fetal surveillance from 39 weeks' gestation to reduce stillbirth in South Asian-born women. *American Journal of Obstetrics and Gynecology* **229**, 286. e281-286. e289 (2023).
23 Schumacher, B., Pothof, J., Vijg, J. & Hoeijmakers, J. H. The central role of DNA damage in the ageing process. *Nature* **592**, 695-703 (2021).
24 Knupp, D. & Miura, P. CircRNA accumulation: A new hallmark of aging? *Mech Ageing Dev* **173**, 71-79 (2018). https://doi.org/doi:10.1016/j.mad.2018.05.001
25 Hall H, M. P., Cooper DA. et al. . Transcriptome profiling of aging Drosophila photoreceptors reveals gene expression trends that correlate with visual senescence. *BMC Genomics* **18** (2017). https://doi.org/https://doi.org/10.1186/s12864-017-4304-3
26 Jeck, W., Sorrentino, J., Wang, K., Slevin, M., Burd, C. *et al.* Circular RNAs are abundant, conserved, and associated with ALU repeats. *RNA* **19**, 141-157 (2013). https://doi.org/doi:10.1261/rna.035667.112.
27 Rybak-Wolf, A., Stottmeister, C., Glažar, P., Jens, M., Pino, N. *et al.* Circular RNAs in the mammalian brain are highly abundant, conserved, and dynamically expressed. *Molecular cell* **58**, 870-885 (2015).
28 Bachmayr-Heyda, A., Reiner, A. T., Auer, K., Sukhbaatar, N., Aust, S. *et al.* Correlation of circular RNA abundance with proliferation–exemplified with colorectal and ovarian cancer, idiopathic lung fibrosis and normal human tissues. *Scientific reports* **5**, 8057 (2015).
29 Song, X., Zhang, N., Han, P., Moon, B.-S., Lai, R. K. *et al.* Circular RNA profile in gliomas revealed by identification tool UROBORUS. *Nucleic acids research* **44**, e87-e87 (2016).
30 Mayhew, T. & Simpson, R. Quantitative evidence for the spatial dispersal of trophoblast nucleic in human placental villi during gestation. *Placenta* **15**, 837-844 (1994).
31 Huppertz, B., Frank, H.-G., Reister, F., Korr, H. & Kaufmann, P. Apoptosis cascade progresses during turnover of human trophoblast: analysis of villous cytotrophoblast and syncytial fragments in vitro. *Laboratory investigation; a journal of technical methods and pathology* **79**, 1687-1702 (1999).
32 Chuprin, A., Gal, H., Biron-Shental, T., Biran, A., Amiel, A. *et al.* Cell fusion induced by ERVWE1 or measles virus causes cellular senescence. *Genes & development* **27**, 2356-2366 (2013).
33 Goldman-Wohl, D. & Yagel, S. United we stand not dividing: the syncytiotrophoblast and cell senescence. *Placenta* **35**, 341-344 (2014).
34 Wang, J., Wang, C., Wei, Y., Zhao, Y., Wang, C. *et al.* Circular RNA as a potential biomarker for forensic age prediction. *Frontiers in Genetics* **13**, 29 (2022).
35 Cheng, J., Huang, J., Yuan, S., Zhou, S., Yan, W. *et al.* Circular RNA expression profiling of human granulosa cells during maternal aging reveals novel transcripts

associated with assisted reproductive technology outcomes. *PLoS ONE* **12**, e0177888 (2017). https://doi.org/https://doi.org/10.1371/journal.pone.0177888

36 Haque, S., Ames, R. M., Moore, K., Pilling, L. C., Peters, L. L. *et al.* circRNAs expressed in human peripheral blood are associated with human aging phenotypes, cellular senescence and mouse lifespan. *GeroScience* **42**, 183-199 (2020). https://doi.org/10.1007/s11357-019-00120-z

37 Akhter, R. in *Circular RNAs* (ed J Xiao) (Springer Nature, 2018).

38 Smith, M. A., Sayre, L. M., Monnier, V. M. & Perry, G. Radical AGEing in Alzheimer's disease. *Trends in neurosciences* **18**, 172-176 (1995).

39 Conn, V. M., Hugouvieux, V., Nayak, A., Conos, S. A., Capovilla, G. *et al.* A circRNA from SEPALLATA3 regulates splicing of its cognate mRNA through R-loop formation. *Nature Plants* (2017).

40 Sun, M. & Yang, Y. Biological functions and applications of circRNAs-next generation of RNA-based therapy. *J Mol Cell Biol* **15** (2023). https://doi.org/10.1093/jmcb/mjad031

41 Woodruff, R., Parekh, F., Lamb, K., Mekkaoui, L., Allen, C. *et al.* Large-scale manufacturing of base-edited chimeric antigen receptor T cells. *Mol Ther Methods Clin Dev* **31**, 101123 (2023). https://doi.org/10.1016/j.omtm.2023.101123

42 Shen, L., Yang, J., Zuo, C., Xu, J., Ma, L. *et al.* Circular mRNA-based TCR-T offers a safe and effective therapeutic strategy for treatment of cytomegalovirus infection. *Mol Ther* **32**, 168-184 (2024). https://doi.org/10.1016/j.ymthe.2023.11.017

43 He, A. T., Liu, J., Li, F. & Yang, B. B. Targeting circular RNAs as a therapeutic approach: current strategies and challenges. *Signal Transduction and Targeted Therapy* **6**, 185 (2021). https://doi.org/10.1038/s41392-021-00569-5

44 Frim, D., Emanuel, R., Robinson, B., Smas, C., Adler, G. *et al.* Characterization and gestational regulation of corticotropin-releasing hormone messenger RNA in human placenta. *The Journal of clinical investigation* **82**, 287-292 (1988).

45 Campbell, E., Linton, E., Wolfe, C., Scraggs, P., Jones, M. *et al.* Plasma corticotropin-releasing hormone concentrations during pregnancy and parturition. *The Journal of Clinical Endocrinology & Metabolism* **64**, 1054-1059 (1987).

46 Sehringer, B., Zahradnik, H., Simon, M., Ziegler, R., Noethling, C. *et al.* mRNA expression profiles for corticotrophin-releasing hormone, urocortin, CRH-binding protein and CRH receptors in human term gestational tissues determined by real-time quantitative RT-PCR. *Journal of molecular endocrinology* **32**, 339-348 (2004).

47 Vasconcelos, S., Moustakas, I., Branco, M. R., Guimarães, S., Caniçais, C. *et al.* Syncytiotrophoblast Markers Are Downregulated in Placentas from Idiopathic Stillbirths. *International Journal of Molecular Sciences* **25**, 5180 (2024).

48 Zhou, Z., Zhang Q, Lu X, Wang R, Wang H, Wang Y-L, Zhu C, Lin H-Y, Wang H. The proprotein convertase furin is required for trophoblast syncytialization. *Cell Death and Disease* **4**, e593 (2013).

49 Overgaard, M. T., Boldt, H. B., Laursen, L. S., Sottrup-Jensen, L., Conover, C. A. *et al.* Pregnancy-associated plasma protein-A2 (PAPP-A2), a novel insulin-like growth factor-binding protein-5 proteinase. *Journal of Biological Chemistry* **276**, 21849-21853 (2001).

50 Morosin, S. K., Delforce, S. J., Corbisier de Meaultsart, C., Lumbers, E. R. & Pringle, K. G. FURIN and placental syncytialisation: a cautionary tale. *Cell Death & Disease* **12**, 635 (2021). https://doi.org/10.1038/s41419-021-03898-z

51 Dauber, A., Muñoz-Calvo, M. T., Barrios, V., Domené, H. M., Kloverpris, S. *et al.* Mutations in pregnancy associated plasma protein A2 cause short stature due to low

IGF-I availability. *EMBO Molecular Medicine* **8**, 363-374 (2016). https://doi.org/https://doi.org/10.15252/emmm.201506106

52 Conover, C. A., Boldt, H. B., Bale, L. K., Clifton, K. B., Grell, J. A. *et al.* Pregnancy-associated plasma protein-A2 (PAPP-A2): tissue expression and biological consequences of gene knockout in mice. *Endocrinology* **152**, 2837-2844 (2011).

53 Cox, L. S. & Redman, C. The role of cellular senescence in ageing of the placenta. *Placenta* **52**, 139-145 (2017).

54 Sultana, Z., Maiti, K., Dedman, L. & Smith, R. Is there a role for placental senescence in the genesis of obstetric complications and fetal growth restriction? *American journal of obstetrics and gynecology* **218**, S762-S773 (2018).

55 McHugh, D. & Gil, J. Senescence and aging: Causes, consequences, and therapeutic avenues. *Journal of Cell Biology* **217**, 65-77 (2018).

56 Baar, M. P., Brandt, R. M., Putavet, D. A., Klein, J. D., Derks, K. W. *et al.* Targeted apoptosis of senescent cells restores tissue homeostasis in response to chemotoxicity and aging. *Cell* **169**, 132-147. e116 (2017).

57 Hannan, N. J., Stock, O., Spencer, R., Whitehead, C., David, A. L. *et al.* Circulating mRNAs are differentially expressed in pregnancies with severe placental insufficiency and at high risk of stillbirth. *BMC Medicine* **18**, 145 (2020). https://doi.org/10.1186/s12916-020-01605-x

58 Mohammed, H., Roberts, C. T., Grzeskowiak, L. E., Giles, L. C., Dekker, G. A. *et al.* Safety and protective effects of maternal influenza vaccination on pregnancy and birth outcomes: A prospective cohort study. *EClinicalMedicine* **26**, 100522 (2020).

59 Byrne, A. B., Arts, P., Ha, T. T., Kassahn, K. S., Pais, L. S. *et al.* Genomic autopsy to identify underlying causes of pregnancy loss and perinatal death. *Nature Medicine* **29**, 180-189 (2023).

60 Drula, R., Braicu, C., Chira, S. & Berindan-Neagoe, I. Investigating circular RNAs using qRT-PCR; roundup of optimization and processing steps. *International Journal of Molecular Sciences* **24**, 5721 (2023).

61 Livak, K. J. & Schmittgen, T. D. Analysis of relative gene expression data using real-time quantitative PCR and the $2^{-\Delta\Delta CT}$ method. *methods* **25**, 402-408 (2001).

Tables and Figures

Table 1. *Characteristics of women and infants from the study by gestational age group (weeks')*

	Gestational Age group (weeks')					Stillbirth
	37	**38**	**39**	**40**	**41+** †	
Maternal age (years)	28.7 ± 1.5	24.1 ± 2.9	25.9 ± 1.9	28.3 ± 4.5	26.8 ± 4.2	#1: 35 #2: 26 #3: 33 #4: 28
Maternal BMI (kg/m^2)	26.4 ± 5.8	27.2 ± 9.1	23.1 ± 4.3	20.8 ± 4.1	23.4 ± 6.2	#1: DM #2: DM #3: DM #4: 22.8
Smoking status*	1/12	2/12	1/12	3/12	2/12	#1: DM #2: DM #3: DM #4: N
Gestational age (weeks)	37.1 ± 0.9	38.0 ± 0.3	39.1 ± 0.7	40.0 ± 0.4	41.5 ± 0.3	#1: 23 #2: 26 #3: 34 #4: 31
Birthweight (g)	2962 ± 325	3345 ± 465	3089 ± 201	3702 ± 161	3513 ± 277	#1: 256 #2: 800 #3: 2546 #4: 1140
Fetal sexˆ	XX = 6 XY = 6	XX = 6 XY = 6	XX = 7 XY = 5	XX = 6 XY = 6	XX = 6 XY = 6	#1: XX #2: XY #3: XY #4: XX

Data are presented as mean ± standard error of the mean.
DM = Data Missing, as data were not available at the time of sample collection.
**** Smoking status as self-reported by patient at time of delivery. X/12 indicates the number of women who reported YES to smoking while pregnant out of the total 12 women. For stillbirths, Y = Yes, N = No.***
ˆ Where XX = female, XY = male.
† The group "41+ weeks' gestation" is defined as delivery at 41+0 through to 41+6 weeks' gestation.

Table 2. *Primer sequences and melt temperatures (T_m) used for qPCR*

Gene	Transcript	Forward primer	Reverse primer	T_m
CRHR2	XM_024446665.1	ATGGACGCGGCACTGCT	ACTGCAGCCTGGCGCT	57
	XM_017011752.2	TCCTACTGCAACACGACCTT	GTTGATCTTTGAGGCCCACG	59
	NM_001202483.2	AGAAAGAGATGTGTGCCAAGC	CCAGAGGAAGAAGGTGGAGG	58
	NM_001202482.2	CTCACTCTCGCGTCCACTC	GTTGATCTTTGAGGCCCACG	59
	NM_001202481.1	GGTCAAATGGGAAGAGAGCC	GTGTTGTACTTGACGCCGTT	58
	NM_001202475.1	CATGACCCTCACCAACCTCT	AAGGTCGTGTTGCAGTAGGA	58
	Circular: circ_0009000	TGGCTACAATTCCTGCTCCA	ACATCTGCTGCTTTGTGTGG	59
CWF19L2	XM_017017239.2	AGATGGTGGATTAAGCTGGCT	GAATGGACTCACGCTCTGGA	59
	XR_947795.2	CCAGAAAGGGAGTATGAACAAAC	CCATGTCACCCACTTCCTTG	57
	NM_152434.3	AGCCATCGGAAACCAGTACT	CCATGTCACCCACTTCCTTG	58
	XM_011542620.3	TCATGGAGTCGCTCTGATGG	ACATCAGGGAATGGGCTCTT	58
	Circular: circ_0024157	AGAAGTGATATACCATTCTTAAATGTA	GATAAATTACAAAATTACATGGATAA	53
RAB22A	NM_020673.3	TATTGTGTGGCGGTTTGTGG	TCTTGTCCAGCTGTATCCCA	58
	Circular: circ_0061017	CCCATTGGCTGAACTCTTCC	AGCCACTACACTTGTTCTTGA	57
FURIN	NM_001382622.1	GCATCATCGACATCCTCACC	GTCTCCACGTCATTCTCGGT	58
	NM_002569.4	ACATCCTCACCGAGCCCA	GACTCTCGGCTGCTCTGG	59
	NM_001382619.1	GTGCAGTCCTCCCTCGAC	TCACTCCTCGATGCCAGAAG	59
	NM_001289823.2	CGGTCGCCTGGAAAAGTT (distinguished by product size)	CTGGACGATGGCATCGAGA	58
	NR_168464.1			
	NM_001382620.1	GACTCGGGTGCGGGATC	TGTTGCTGCTACCACCCATA	58
	NM_001382621.1	CCAAGAACACAGCCAGGAAG	TACCACCCATAGCAACCAGG	58
	NM_001289824.2	GGTTTGAGACAAACTGGGACTAG	GACCAAGGTTCCTGTTGCTG	58
	Circular: circ_0036877	TTTGTAAGATGCTGGGTTGGTG	ACTGCATCTGTCACCTCGC	57

Gene	Transcript	Forward primer	Reverse primer	T_m
PNPT1	NM_033109.5	CCTTCCCAGTTTATGCCTTTGG	AAAGAGCGGTCTAATTGAACGAT	60
	Circular: circ_0054624	AGCATGTTAGGCAATGTTGAT	TTTACTGACCGCTGTGACCA	60
PAPPA2	XM_005245422.3	GCATCTCAGCTGTGGCTCTA	AGTTACTGGGAGCCGAAAGAC	56
	Circular: circ_0111277	AGTCGATGGATTCCTCTCAT	AAGTTGTTCATCACTCTGTT	55
YWHAZ		ACCGTTACTTGGCTGAGGTTGC	CCCAGTCTGATAGGATGTGTTGG	60
GAPDH		TCAAGGCTGAGAACGGGAAG	CGCCCCACTTGATTTTGGAG	60
ACTINB		CACCATTGGCAATGAGCGGTTC	AGGTCTTTGCGGATGTCCACGT	60
CXCL8		AAGCTGGCCGTGGCTCTCTTG	AGCCCTCTTCAAAAACTTCTC	60
CST3		CAACAAAGCCAGCAACGACA	TCTTGGTACACGTGGTTCGG	60
TYROBP		ACTGAGACCGAGTCGCCTTAT	ATACGGCCTCTGTGTGTTGAG	61
FCER1G		AGCAGTGGTCTTGCTCTTACT	TGCCTTTCGCACTTGGATCTT	62
LYZ		CTTGTCCTCCTTTCTGTTACGG	CCCCTGTAGCCATCCATTCC	60
CCL3		TTCTCTGTACCATGACACTCTGC	CGTGGAATCTTCCGGCTGTAG	61
CTSS		CCATTGGGATCTCTGGAAGAAAA	TCATGCCCACTTGGTAGGTAT	59
AIF1		ATCAACAAGCAATTCCTCGATGA	CAGCATTCGCTTCAAGGACATA	60
HMGA1		GCTGGTAGGGAGTCAGAAGGA	TGGTGGTTTTCCGGGTCTTG	62
HIRA		TTCAGTTGATATTCACCCTGACG	AAGTGATTGTCCATCTGGCAAA	59

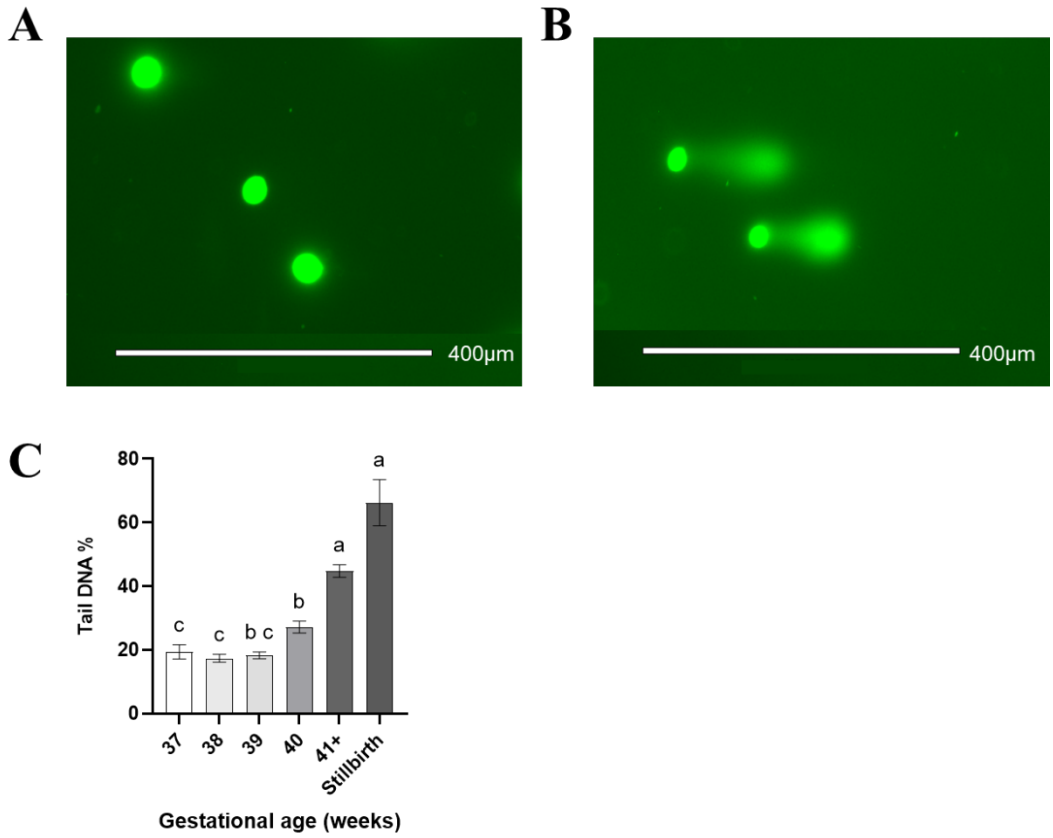

Figure 1. *Representative images of* ***(A)*** *healthy cells and* ***(B)*** *DNA damaged cells, as imaged using epifluorescent microscopy after performing a Comet Assay.* ***(C)*** *Levels of DNA damage, as assessed by Tail DNA %, in isolated cells from 37, 38, 39, 40 and 41+ uncomplicated, and stillbirth, placentae. n = 12 placentae / uncomplicated gestational group, n = 4 stillbirth placentae. 100 cells analysed following Comet Assay, per placenta. Data are presented as mean ± standard error of the mean. Different letters represent statistically significant (p < 0.05) differences.*

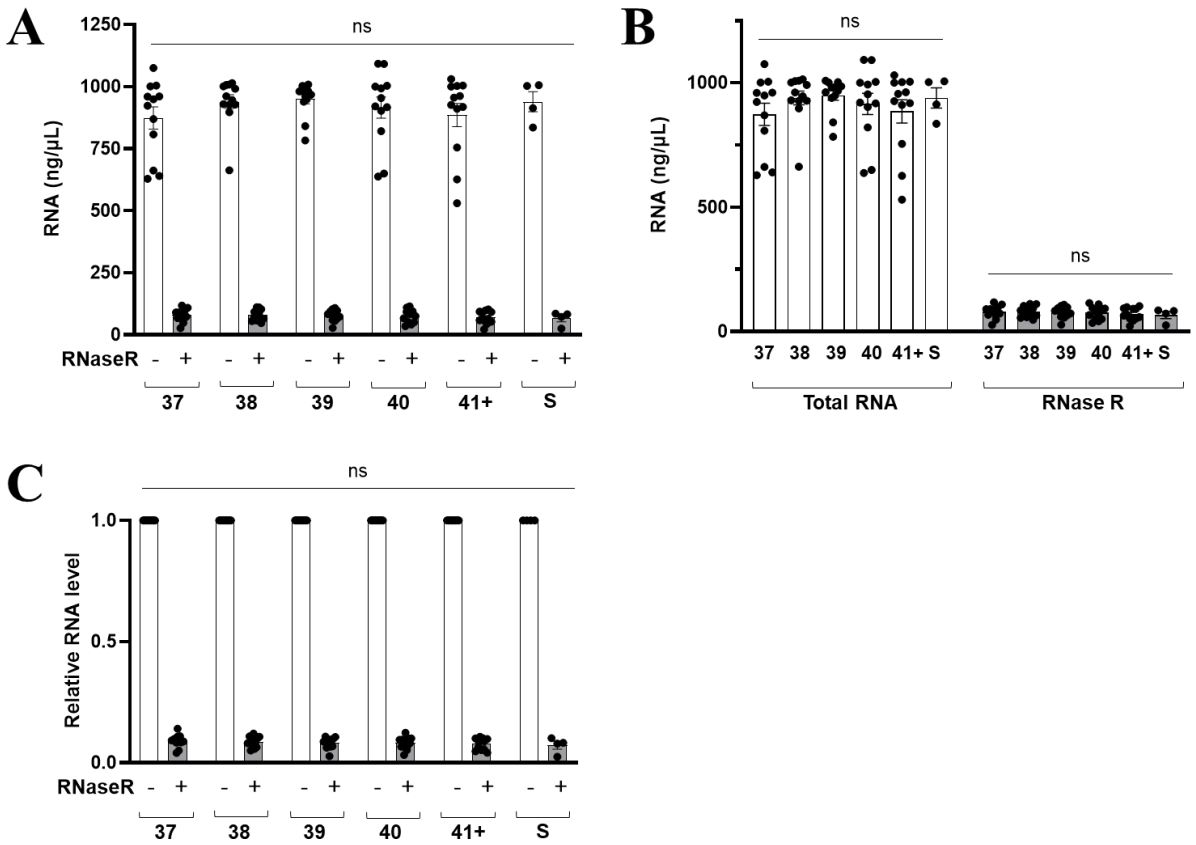

Figure 2. (A-B) *RNA concentration (ng / µL) and* ***(C)*** *abundance (as fold change of RNase R-depleted RNA relative to total RNA) in isolated cells from 37, 38, 39, 40 and 41+ uncomplicated, and stillbirth (S), placentae. n = 12 placentae / uncomplicated gestational group, n = 4 stillbirth placentae. Data are presented as scatter plots with bars and indicate mean ± standard error of the mean. ns = not significant.*

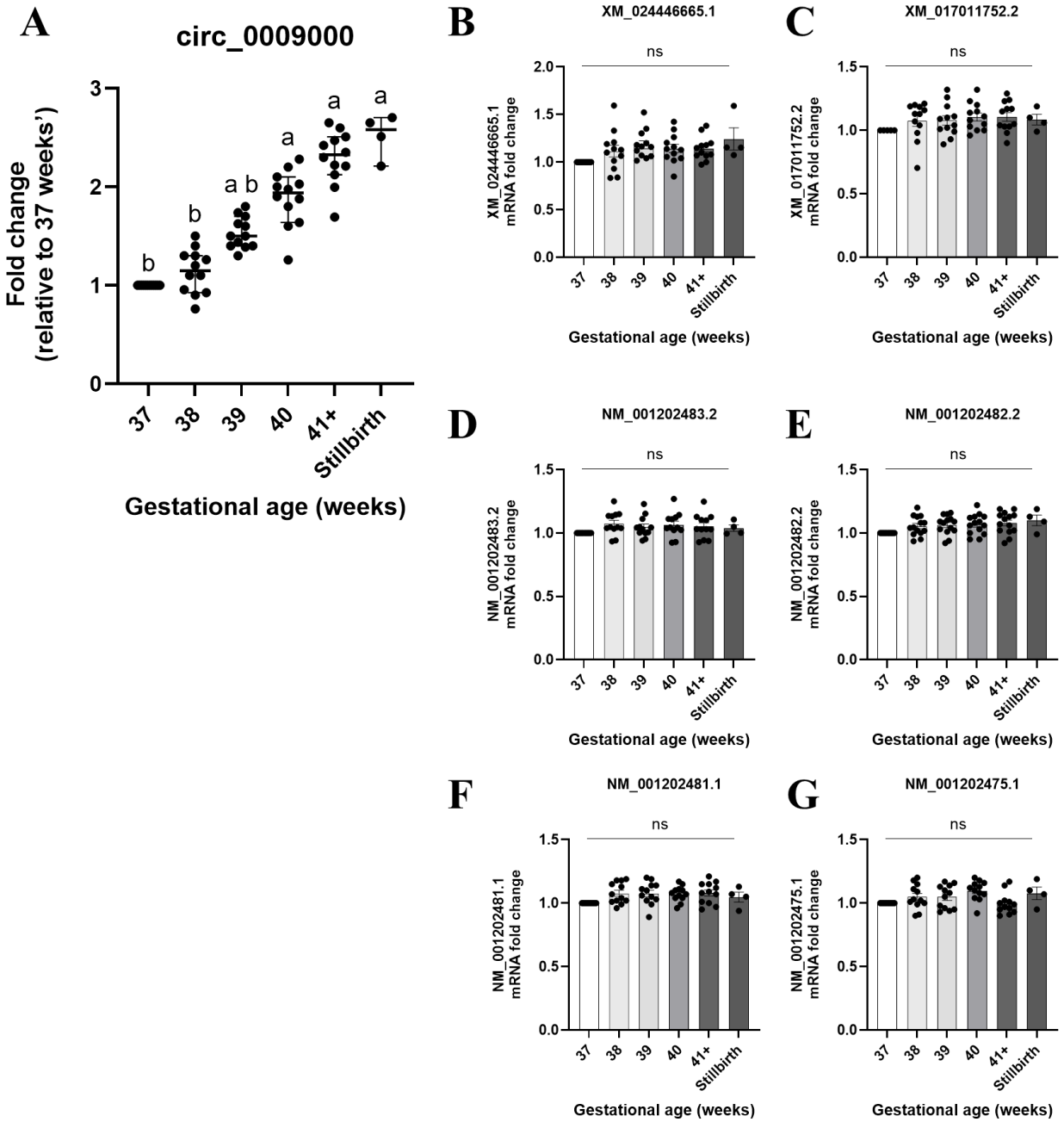

Figure 3. *Abundance (as fold change relative to abundance at 37 weeks' gestation) of* ***(A)*** *circ_0009000 and linear CRHR2 gene variants* ***(B)*** *XM_024446665.1,* ***(C)*** *XM_017011752.2,* ***(D)*** *NM_001202483.2,* ***(E)*** *NM_001202482.2,* ***(F)*** *NM_001202481.1 and* ***(G)*** *NM_001202475.1, in isolated cells from 37, 38, 39, 40 and 41+ uncomplicated, and stillbirth, placentae. n = 12 placentae / uncomplicated gestational group, n = 4 stillbirth placentae. Data are presented as scatter plots with bars, and indicate mean ± standard error of the mean. Different letters represent statistically significant (p < 0.05) differences. ns = not significant.*

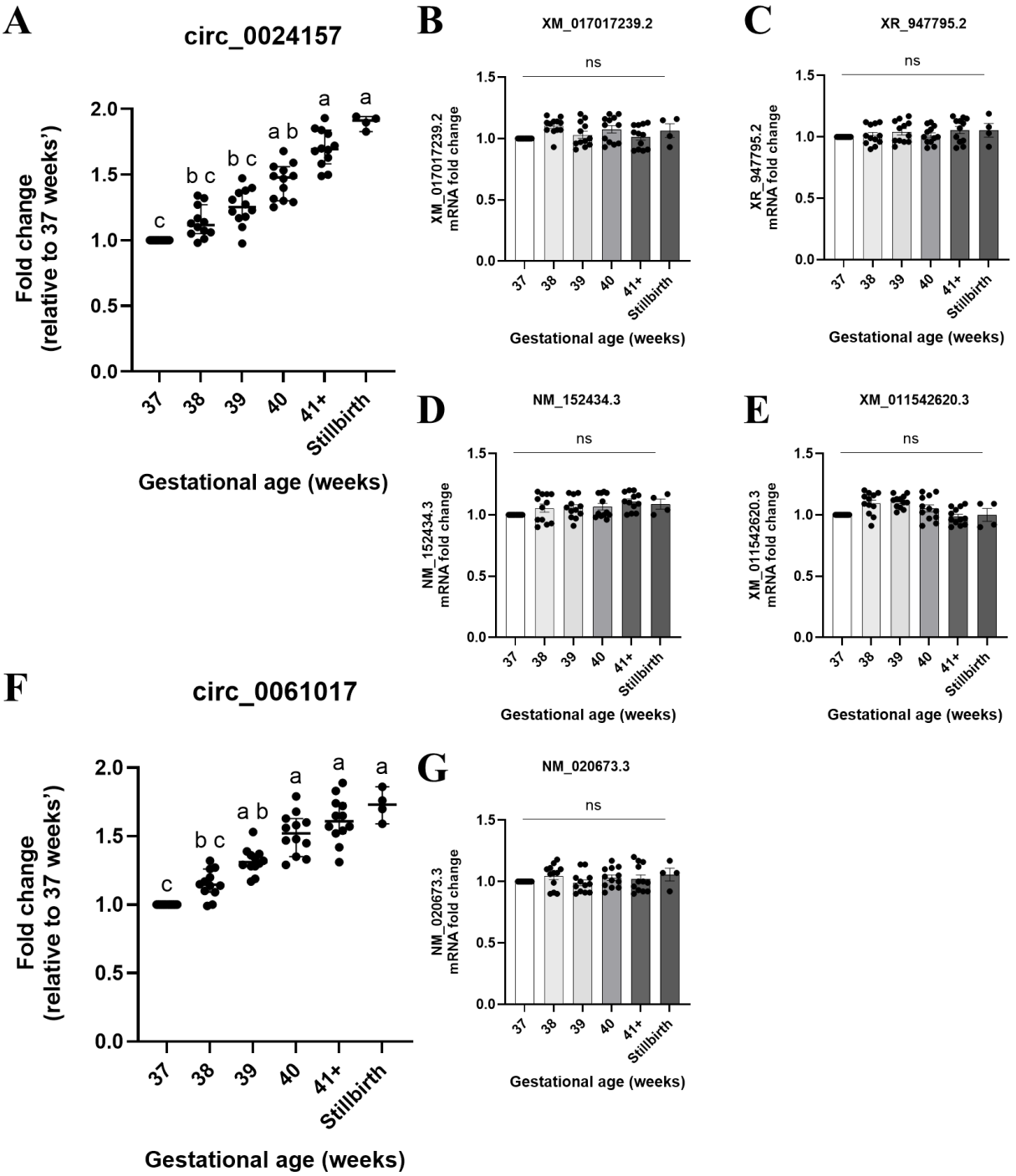

Figure 4. *Abundance (as fold change relative to abundance at 37 weeks' gestation) of* ***(A)*** *circ_0024157 and linear CWF19L2 gene variants* ***(B)*** *XM_017017239.2,* ***(C)*** *XR_947795.2,* ***(D)*** *NM_152434.3 and* ***(E)*** *XM_011542620.3. Abundance (as fold change relative to abundance at 37 weeks' gestation) of* ***(F)*** *circ_0061017 and linear RAB22A gene variant* ***(G)*** *NM_020673.3; all in isolated cells from 37, 38, 39, 40 and 41+ uncomplicated, and stillbirth, placentae. n = 12 placentae / uncomplicated gestational group, n = 4 stillbirth placentae. Data are presented as scatter plots with bars, and indicate mean ± standard error of the mean. Different letters represent statistically significant (p < 0.05) differences. ns = not significant.*

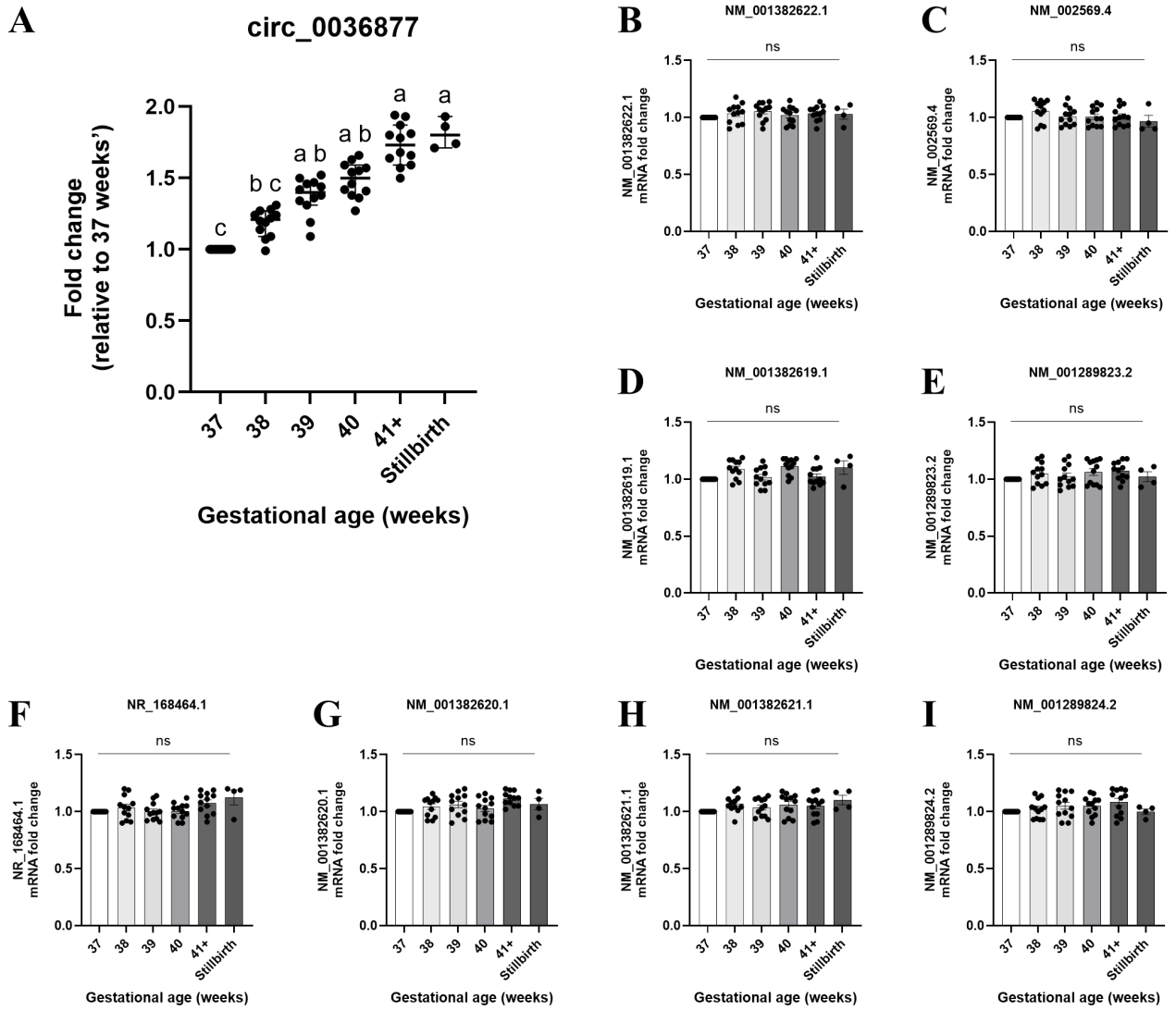

Figure 5. *Abundance (as fold change relative to abundance at 37 weeks' gestation) of* ***(A)*** *circ_0036877 and linear FURIN gene variants* ***(B)*** *NM_001382622.1,* ***(C)*** *NM_002569.4,* ***(D)*** *NM_001382619.1,* ***(E)*** *NM_001289823.2,* ***(F)*** *NR_168464.1,* ***(G)*** *NM_001382620.1,* ***(H)*** *NM_001382621.1 and* ***(I)*** *NM_001289824.2 in isolated cells from 37, 38, 39, 40 and 41+ uncomplicated, and stillbirth, placentae. n = 12 placentae / uncomplicated gestational group, n = 4 stillbirth placentae. Data are presented as scatter plots with bars, and indicate mean ± standard error of the mean. Different letters represent statistically significant (p < 0.05) differences. ns = not significant.*

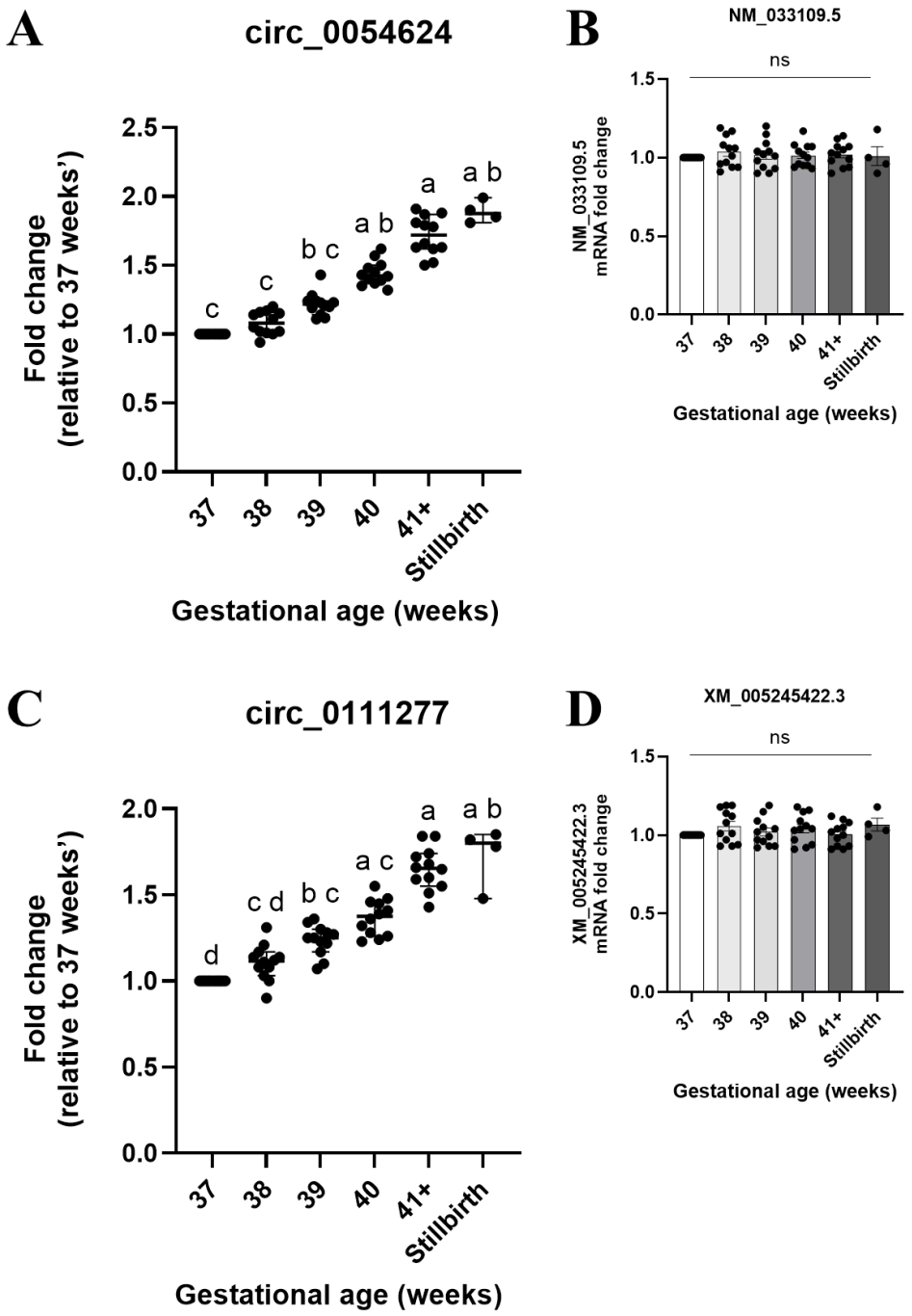

Figure 6. *Abundance (as fold change relative to abundance at 37 weeks' gestation) of* ***(A)*** *circ_0054624 and linear PNPT1 gene variant* ***(B)*** *NM_033109.5. Abundance (as fold change relative to abundance at 37 weeks' gestation) of* ***(C)*** *circ_0111277 and linear PAPPA2 gene variant* ***(D)*** *XM_005245422.3; all in isolated cells from 37, 38, 39, 40 and 41+ uncomplicated, and stillbirth, placentae. n = 12 placentae / uncomplicated gestational group, n = 4 stillbirth placentae. Data are presented as scatter plots with bars, and indicate mean ± standard error of the mean. Different letters represent statistically significant (p < 0.05) differences. ns = not significant.*

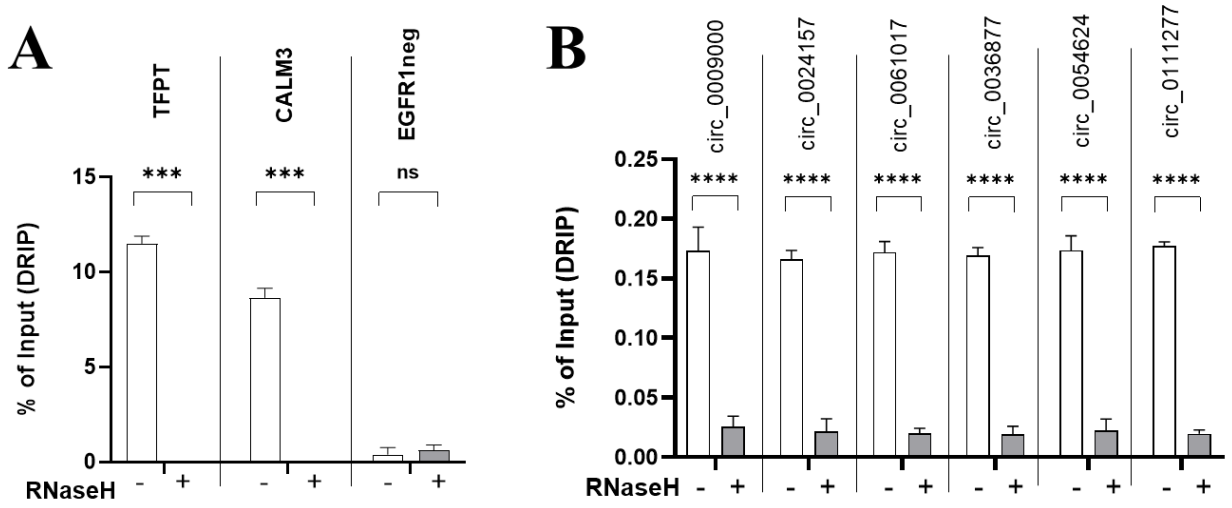

Figure 7. *DRIP-qPCR analysis using primers for* ***(A)*** *R-loop-positive loci TFPT and CALM3, and R-loop-negative locus EGFR1neg, and* ***(B)*** *circ_0009000, circ_0024157, circ_0061017, circ_0036877, circ_0054624 and circ_0111277. Where indicated, samples were treated with RNase H prior to DRIP. Treatment with RNase H significantly suppressed the DRIP-qPCR signal, consistent with R-loop formation in the tested regions. DRIP-qPCR signal intensity shown as % of Input (DRIP), with indication of mean ± standard error of the mean. *** $p < 0.001$, **** $p < 0.0001$, ns = not significant. n = 5 placentae with, and n = 5 placentae without, RNase H treatment.*

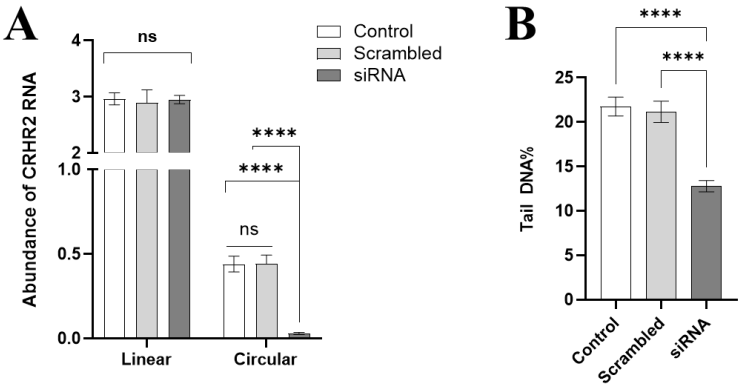

Figure 8. (A) *Abundance of CRHR2 mRNA ("linear") and circ_0009000 ("circular"), and* ***(B)*** *Levels of DNA damage, as assessed by Tail DNA %, in HEK293T cells, either untransfected ("control"), transfected with a scrambled siRNA ("scrambled") or transfected with an siRNA specific to circ_0009000 ("siRNA"). n = 9 / group. 100 cells analysed following Comet Assay, per group. Data are presented as mean ± standard error of the mean. **** $p < 0.0001$, ns = not significant.*

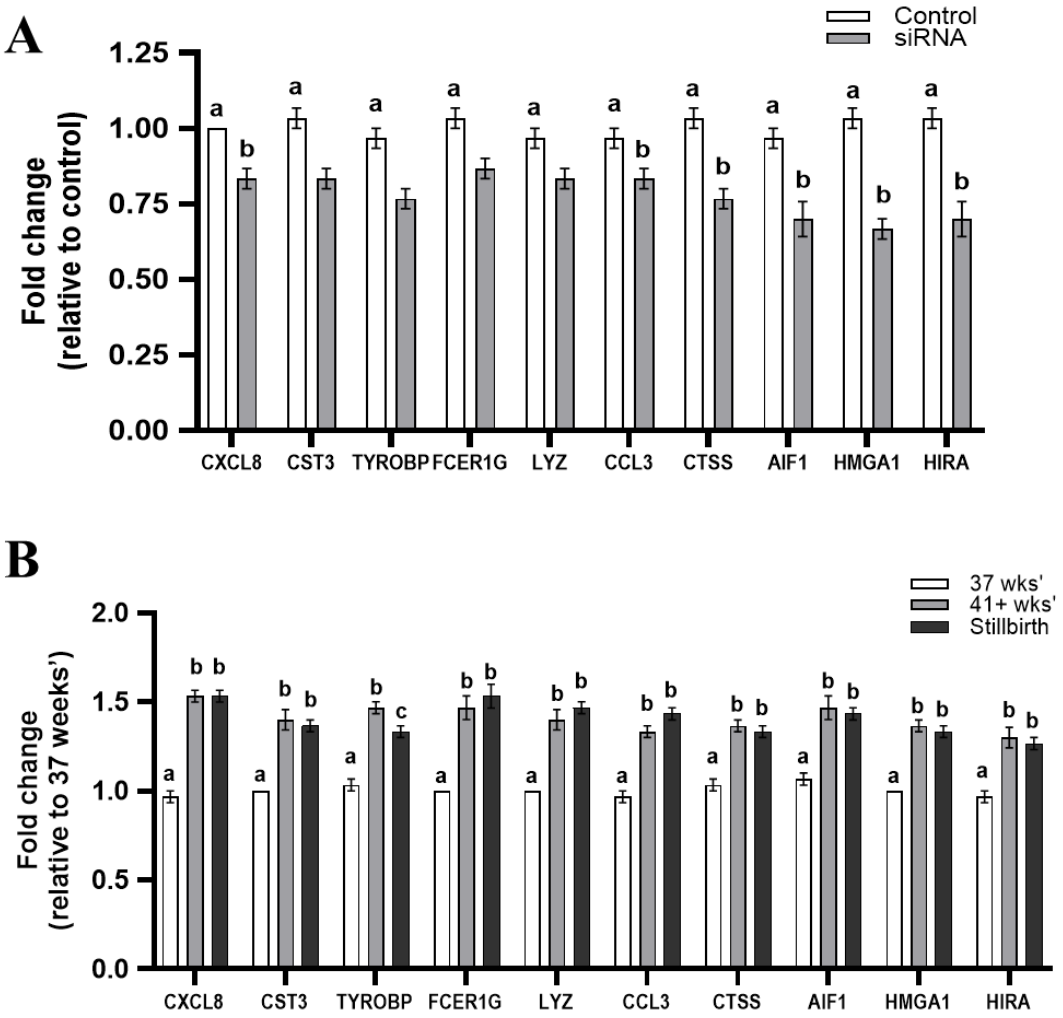

Figure 9. *Fold change mRNA expression of senescence-associated genes in* ***(A)*** *HEK293T cells treated with siRNA specific to circ_0009000 (grey) or HEK293T cells treated with control (white), and* ***(B)*** *placenta tissue from 37 weeks' gestation uncomplicated pregnancy (white), 41+ weeks' gestation uncomplicated pregnancy (grey) or stillbirth (black). For* ***(A)*** *n = 9 / group, for* ***(B)*** *n = 12 placentae / uncomplicated gestational group, n = 4 stillbirth placentae. Data are presented as mean ± standard error of the mean. Different letters represent statistically significant (p < 0.05) differences. ns = not significant.*

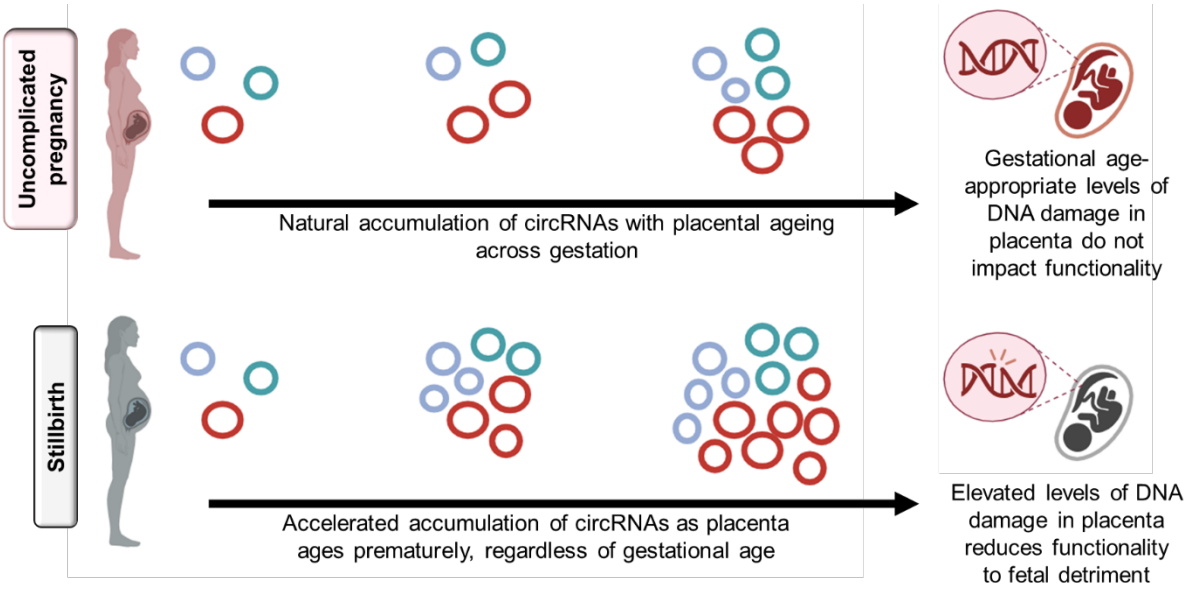

Figure 10. *Proposed mechanism by which circRNA accumulation and placental ageing contribute to stillbirth.*